JACS
JOURNAL OF THE AMERICAN CHEMICAL SOCIETY

ARTICLE

pubs.acs.org/JACS

Oxidatively Induced Concurrent Cationic and Radical Polymerization of Isobutylene in the Presence of $LiCB_{11}Me_{12}$

Victoria Volkis,[†,‡] Christos Douvris,[†] and Josef Michl*[,†,§]

[†]Department of Chemistry and Biochemistry, University of Colorado, Boulder, Colorado 80309-0215, United States

[§]Institute of Organic Chemistry and Biochemistry, Academy of Sciences of the Czech Republic, 16610 Prague 6, Czech Republic

Supporting Information

ABSTRACT: A solution of a mechanistic puzzle is reported: upon initiation with air at 25 °C or with di-*tert*-butyl peroxide at 80 °C, isobutylene (IB) polymerizes at 1 atm in weakly coordinating solvents containing 10 wt % $LiCB_{11}(CH_3)_{12}$ to a mixture of highly branched (*b*-PIB) and linear (*l*-PIB) polyisobutylene. The former polymer is separable by solvent extraction and is identical with the *b*-PIB that is produced from IB as a sole product under similar conditions under nonoxidizing radical initiation with azo-*tert*-butane. The latter polymer differs from standard *l*-PIB in that it carries a carborane anion attached at the chain end. The molecular weight of *b*-PIB ranges up to 26 000, and that of *l*-PIB, up to 50 000. Evidence is presented that the concurrent polymerization of IB to *b*-PIB and *l*-PIB is launched by an initial oxidation of the $CB_{11}(CH_3)_{12}^-$ anion to a neutral radical $CB_{11}(CH_3)_{12}^{\bullet}$. This radical is proposed to subsequently transfer a methyl radical to IB, thus launching the formation of *b*-PIB by the radical mechanism while leaving behind the borenium ylide $CB_{11}(CH_3)_{11}$, which is a strong Lewis acid and induces simultaneously the formation of *l*-PIB by the cationic mechanism.

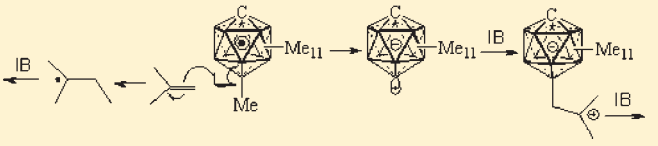

INTRODUCTION

A few years ago we reported that radical homopolymerization of simple alkenes can be induced by the presence of high concentrations of lithium dodecamethylmonocarba-*closo*-dodecaborate, $LiCB_{11}(CH_3)_{12}$ (**1**, Chart 1),[1] and a radical source such as air. This observation raised interesting mechanistic questions. For example, for unactivated alkenes containing allylic hydrogens the radical mechanism is normally suppressed by chain transfer to monomer, and oxygen is ordinarily viewed as a radical polymerization inhibitor, not an initiator. We have since discovered that the reaction outcome is a quite sensitive function of the exact reaction conditions and can be strongly affected by the presence of impurities or additives. For instance, the small amount of sulfolane that usually remains in **1** from its synthesis even after considerable purification is crucial for its catalytic activity, and rigorously purified **1** is inactive. We now believe that the solutions of **1** in solvents of low polarity are colloidal and that the activity of Li^+ ions in such solutions is strongly affected by aggregation, which has long been known[2] to be sensitive to small amounts of impurities and additives. Although cursory examination of several other alkylated CB_{11} carborate anions revealed similar behavior, our efforts to find other types of lithium salts that would act as similar catalysts have so far remained unsuccessful.

The polymerization of isobutylene (IB) was particularly intriguing, since its six allylic hydrogens normally make chain transfer to monomer especially facile. A closer investigation confirmed that, in the presence of **1** in weakly coordinating solvents and with initiation under nonoxidizing conditions, radical polymerization of IB indeed takes place.[3] This outcome was rationalized by noting

Chart 1. Structure of 1 and Structures 2−5 Deduced from MALDI-TOF in C_{60} Matrix (Table 4, run 1)

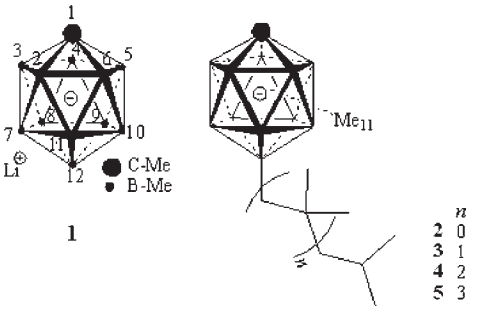

1

that even if the rate of allylic abstraction and resulting chain transfer remain as high as usual, a rate of propagation that has been increased sufficiently by complexation of IB to Li^+ will make chain growth competitive. The complexation to Li^+ then has a function similar to that of the methoxycarbonyl substituent in methacrylate, whose radical polymerization is not suppressed by allylic abstraction either.

The radical process produces a polyisobutylene (*b*-PIB) with a degree of polymerization up to ~500, whose structure is extremely highly branched, unlike any previously reported for PIB. It is believed to be best represented as $[\text{-CHR-}]_n$, where R is

Received: December 27, 2010
Published: May 04, 2011

dx.doi.org/10.1021/ja111659u | *J. Am. Chem. Soc.* 2011, 133, 7801–7809

most often equal to $-C(CH_3)_2[CH_2C(CH_3)_2]_3CH_2CH(CH_3)_2$. The properties of *b*-PIB are very different from those of the ordinary linear polyisobutylene (*l*-PIB, $[-CH_2C(CH_3)_2-]_n$). The latter is produced on an industrial scale by low-temperature cationic polymerization of IB, which requires a strong Lewis acid and a temperature well below 0 °C.[4−7]

Catalysis with **1** can also be used for radical copolymerization of IB with ethyl acrylate.[3,8] Most recently we have examined in more detail the radical polymerization of propene, which produces highly branched polypropylene.[9] In contrast, 1-hexene and 1-octene yield only relatively low molecular weight oligomers under the conditions used recently.[10] Admittedly, until the detailed composition of the presumably colloidal catalytic solutions containing **1** in solvents of low polarity is better understood, it will be difficult to control these polymerization reactions.

Presently, we propose a solution to an intriguing mechanistic puzzle, the polymerization of IB in weakly coordinating solvents containing **1** and an oxidizing initiator, di-*tert*-butyl peroxide (DTPB) or oxygen. Under these conditions, even at temperatures as high as 80 °C, IB polymerizes to a mixture of *b*-PIB (M_w = 1000−26 000) and *l*-PIB (M_w up to ∼50 000), which carries the carborate anion as one of the chain ends. The molecular weight of the resulting *l*-PIB is amazingly high, considering the elevated temperature at which the reaction is performed. How can oxygen act as an initiator, and how does a single initiator simultaneously launch the production of two different polymers from the same IB monomer?

EXPERIMENTAL SECTION

General. All manipulations with air-sensitive materials were carried out with the rigorous exclusion of oxygen and moisture (except in the case of air-initiated polymerization) in a dual manifold Schlenk line, equipped with an air-free vacuum pump with a vacuum range $(1-3) \times 10^{-4}$ Torr. Argon was purified by passage through a MnO oxygen-removal column and a Davison 4 Å molecular sieve column. All chemicals were reagent grade and were used as purchased (Aldrich). All solvents were anhydrous grade. $Me_3NHCB_{11}H_{12}$ was purchased from Katchem Ltd. (Prague, Czech Republic) or synthesized by a published procedure.[11] A sample of *l*-PIB (BASF 2300) was obtained from BASF, and on our gel-permeation chromatograph (GPC) showed a (relative) M_w of 4000. Sulfolane and acetone-d_6 were dried with activated Davison 4 Å molecular sieves. 1,2-Dichloroethane (DCE), dichloromethane, and 1,1,2,2-tetrachloroethane (TCE) were dried with calcium hydride and then distilled under argon. Tetrahydrofuran, benzene, and toluene were distilled from sodium benzophenone. All other solvents were freshly distilled before use.

NMR spectra of PIB were measured at room temperature (RT) in chloroform-*d* unless stated otherwise. ^{11}B NMR spectra were measured with a Varian XRS-300 spectrometer at 96.2 MHz. ^{1}H, ^{2}H, and indirectly observed two-dimensional NMR spectra [gradient correlation spectroscopy (gCOSY) and gradient heteronuclear single and multiple quantum coherence spectroscopy (gHSQC and gHMQC) with boron decoupling] were measured with a Varian Unity-500 spectrometer equipped with a Nalorac IDTXG-500-5 indirect triple-resonance probe at 500 and 160.4 MHz, respectively. ^{13}C, distortionless enhancement by polarization transfer (DEPT), and diffusion-ordered spectroscopy (DOSY) spectra were measured with a Varian XRS-400 spectrometer. Electrospray ionization mass spectrometry (ESI-MS) spectra were recorded with a Hewlett-Packard 5989 mass spectrometer. Matrix-assisted laser desorption ionization time-of-flight (MALDI-TOF) spectra were recorded with a Voyager DE STR TM spectrometer.

Thermogravimetric analysis (TGA) and differential scanning calorimetry (DSC) were performed under nitrogen on TGA Q500 and DSC Q500 instruments (TA Instruments−Waters LLC), respectively, with heating rates of 10 °C/min. Sample size for the TGA was 10−20 mg and for the DSC, 5 mg (representative examples are shown in Figures S1 and S2 in Supporting Information).

Size-Exclusion Chromatography. Most molecular weight determinations, including all those listed in the tables, were performed on a Waters gel permeation chromatograph, with refractive index detector (RI 2414 in a channel signal inversion mode) and EMPOWER software, with a three-column bed (Styragel HR 4.6 300 mm columns for molecular weight ranges 100−10 000, 500−30 000, and 5000−6 000 000) and a flow rate of 0.3 mL/min. These molecular weights were evaluated by comparison with polystyrene standards from Aldrich and therefore are only relative. Most GPC traces showed two overlapping peaks, due to *l*-PIB and *b*-PIB, and signal deconvolution was used to evaluate their molecular weights.

At the end of the project we gained access to a Viscotek GPC instrument consisting of an isocratic pump, vacuum-membrane degasser, nonthermostatic auto sampler, set of two thermostated columns (Viscotek G4000 and G6000), and a triple detection system including a refractive index (RI) detector, a light scattering (LS) detector with low (7°) and right (90°) angle detection, and an intrinsic viscosity (IV) detector. The mobile phase was tetrahydrofuran (THF; HPLC quality stabilized by Organox 200 ppm) at 1 mL/min. Columns and detectors were at 35 °C. The calibration and calculations were done via the universal method for triple detection. For a narrow polystyrene standard (Viscotek) with M_w = 98 000 in THF solution, d*n*/d*c* was 0.185 mL/g. The exact concentration and dilution were used for the calculation of d*n*/d*c*. Concentrations of samples were 2.5−6 mg/mL. Sample solutions were prepared 24 h prior to measurements in order to achieve full equilibration of the polymer. Data evaluation relied on the original OmniSec software delivered with the instrument. We were able to analyze two representative samples of *l*-PIB from which all *b*-PIB had been removed as described below. Only the two *l*-PIB molecular weights from this determination are absolute.

Molecular Modeling. A B3LYP/6-31G calculation was performed for the proposed carborate-containing chain terminus by use of the Gaussian09 program package.[12]

Lithium Catalyst. The preparation of sulfolane-free and sulfolane-containing $LiCB_{11}Me_{12}$ (**1**) followed reported procedures.[13] A sample of **1** carrying CD_3 groups in positions 2−12 and a CH_3 group in position 1 was prepared in the same way but by use of trideuteriomethyl triflate (Aldrich) in the second step. The catalytic power of **1** is strongly affected by the presence of small amounts of polar additives such as sulfolane, LiCl, triflic acid, and water. Without a polar additive, the catalyst is inactive. Unless otherwise stated, the salt **1** used in this work contained sulfolane in the molar ratio sulfolane: Li^+ = 0.17, which is close to optimal for DCE solution and initiation with DTBP.

Catalyst Regeneration. After a completed polymerization reaction, hot (55 °C) hexane was added to dissolve the polymer. The catalyst was insoluble in hexane and was collected by filtration. It was dissolved in acetonitrile and decolorized with activated charcoal following a previously published[13] procedure. Acetonitrile was evaporated under reduced pressure and the catalyst was kept at 180 °C and 0.01 Torr overnight. Sulfolane was added if necessary to reach the optimal composition, monitored by ^{1}H NMR.

In an attempt to find out more about the fate of the catalyst, air was bubbled for 1 min through a solution of **1** (50 mg) in DCE-d_4 (0.5 mL) in a J-Young NMR tube. The mixture was exposed to 1 atm of IB for 2 weeks at room temperature, and an NMR spectrum was taken occasionally. At the end, C_{60} in DCE (1 mg/mL) was added and the solution was analyzed by MALDI-TOF.

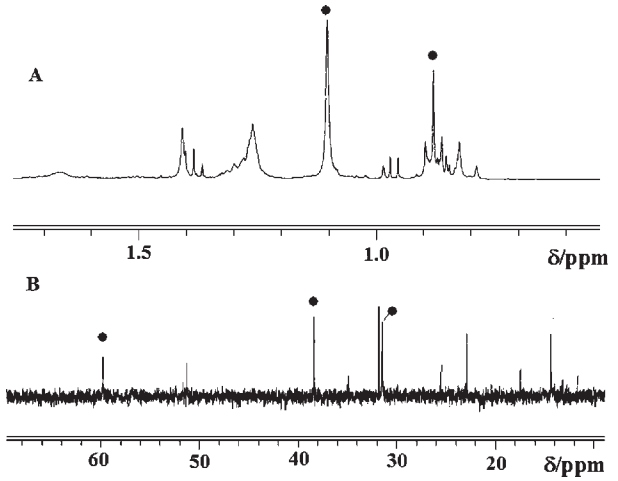

Figure 1. Typical (A) ^{1}H and (B) ^{13}C NMR spectra in $CDCl_3$ of a mixture resulting from polymerization of IB initiated under oxidative conditions. Peaks marked with black dots belong to *l*-PIB and the others to *b*-PIB.

Radical $CB_{11}Me_{12}^{\bullet}$ and Borenium Ylide $CB_{11}Me_{11}$. The radical was synthesized by oxidation of the anion.[13] Its low-temperature reaction with hexa-*tert*-butyldisilane[14] in pentane was used to produce the borenium ylide, which was immediately treated with IB in hexane or liquid SO_2. Polymerization was allowed to proceed below −60 °C for 24 h.

Polymerization of IB and Separation of *l*-PIB. A weighed amount of catalyst was placed in a reactor and dried for 24 h at 0.01 Torr at room temperature, and freshly distilled solvent was added. A typical concentration was 10 wt % **1** relative to solvent. When air was used as the initiator, it was bubbled trough the solution of the catalyst prior to the addition of IB. DTBP was used neat and was added to the solution of the catalyst before the addition of IB. The Schlenk flask was connected to a 1 L glass bulb. The solution in the reactor was frozen, and the reactor and the bulb were evacuated and then filled with IB. The polymerization reactors were connected to a manifold and a differential manometer. IB was refilled periodically to keep the pressure at ∼1 atm. After the reaction was complete, methanol was added and then all solvents were evaporated. PIB was extracted three times with hexane (30 mL) at 45−50 °C. Hexane was evaporated and the PIB was dried in a vacuum oven for 24 h at 100 °C. In some instances Kugelrohr distillation at 10^{-3} Torr was used to separate different polymer and oligomer fractions at 180 °C overnight. To separate *l*-PIB, Kugelrohr distillation was followed by repeated precipation of the nonvolatile residue by pouring a hot hexane solution into cold (∼−20 °C) acetone and filtering the mixture.

RESULTS

Catalyst. Relatively high concentrations of **1**, on the order of 10 wt %, are required for catalytic action. Stable solubility of **1** is ∼20 wt % in DCE and ∼10% wt in benzene. Light scattering observed during an unsuccessful attempt to obtain a Raman spectrum suggests that these solutions are colloidal. Higher concentrations can be achieved, but the initially clear solutions are then not stable indefinitely and ultimately form a precipitate. The catalytic activity of the resulting suspensions is very low.

Under the oxidizing conditions used, some **1** is incorporated into the polymer and only the rest can be recovered. We have reused it up to six times after recovery with no loss in activity. Thus, **1** acts not only as a catalyst but also as a reagent.

Polymerization. As described previously,[3] in the presence of solvent and sulfolane-containing **1** the nonoxidizing initiator, azo-*tert*-butane (ATB), converts IB exclusively to *b*-PIB. This paper presents only results obtained with initiators that are also oxidants, DPTB and air (Tables 1−5). In the absence of other additives, these produce a mixture of *b*-PIB with *l*-PIB, readily identified by their known and characteristic NMR spectra (Figure 1). The relative content of *b*-PIB and *l*-PIB in the mixture was determined by ^{1}H NMR integration and depends sensitively on reaction conditions. The two polymers differ not only in structure but also in molecular weight (M_w), as revealed by GPC (Figure 2).

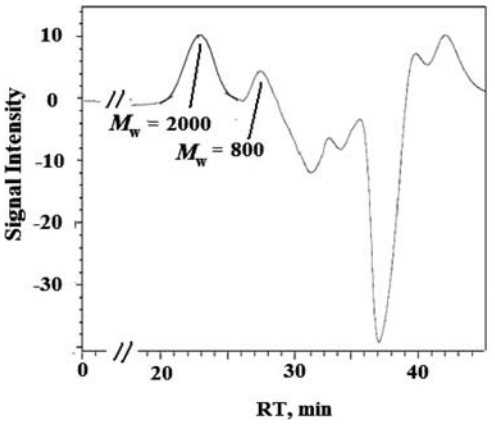

Figure 2. GPC trace of a crude sample from run 3 in Table 3 (automatic inversion mode, polymer peaks shown as positive and system peaks as negative).

Table 1. Effect of Initiator on Polymerization of IB[a]

run	initiator	*T*, °C	PIB, mg[b]	PIB composition[c]	M_w	MWD[d]
1	air	25	60	90% *l*-PIB	32 000	2.7
	air	25	60	10% *b*-PIB	650	1.6
2	DTPB	80	27	80% *l*-PIB	25 000	2.4
	DTPB	80	27	20% *b*-PIB	2000	2.0

[a] DCE (0.5 mL), **1** (50 mg), initiator (50 mg or 1 min bubbling with air), 1 atm of IB, 24 h. [b] Total polymer yield. [c] Determined by ^{1}H NMR integration. [d] Molecular weight distribution.

Thermal analysis of crude unseparated polymer mixtures yields two different T_g points (−28.5 and −9.5 °C, Figure S1 in Supporting Information) and two different decomposition temperatures T_d (227 and 371 °C, Figure S2 in Supporting Information). Comparison with samples of pure *b*-PIB obtained by polymerization under nonoxidizing conditions[3] shows that the thermal properties of the component with T_g = −28.5 °C and T_d = 227 °C are nearly identical to those reported for *b*-PIB. The other component of the mixture, presumably *l*-PIB, has a thermal stability higher than normally observed for *l*-PIB obtained by cationic polymerization. The T_d of our *l*-PIB is ∼370 °C, whereas we measured ∼300 °C on a sample of comparable M_w (∼4000 based on polystyrene standards) obtained from BASF.

High-M_w *l*-PIB and *b*-PIB can be separated fairly well by extraction with methanol, in which the former is poorly soluble. A partial separation of the low-M_w portion of the polymer (oligomer) mixture into several fractions was accomplished by Kugelrohr distillation at 180 °C at 0.01 Torr (Table 1 run 2 and Table 3 run 3). Each fraction was characterized by TGA, DSC, NMR, and GPC. The more volatile oligomeric material is

dx.doi.org/10.1021/ja111659u | *J. Am. Chem. Soc.* 2011, 133, 7801–7809

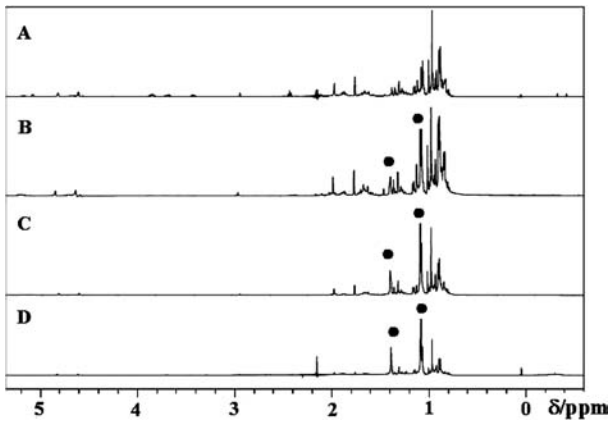

Figure 3. $^{1}H\{^{11}B\}$ NMR spectra in $CDCl_3$ of a fractionated low-M_w PIB sample from run 3 in Table 3. The most volatile fraction A is mostly *b*-PIB, and the least volatile fraction D is mostly *l*-PIB.

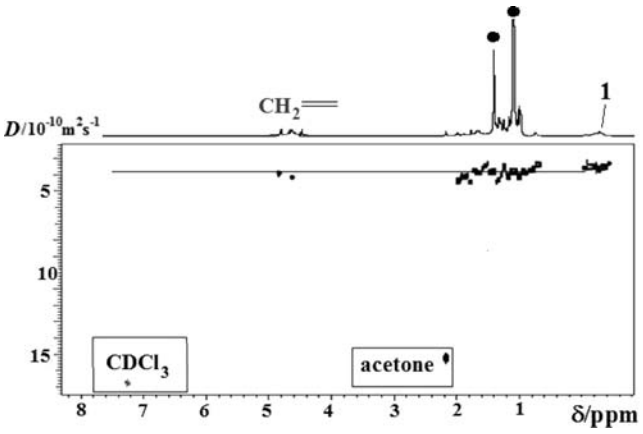

Figure 4. ^{1}H gDOSY NMR spectrum in $CDCl_3$ of the *l*-PIB fraction from run 3 in Table 3. The peaks labeled **1** are not due to free **1** but to a methylated carborate anion attached to a chain end.

predominantly *b*-PIB and the remaining less volatile polymeric material is mostly *l*-PIB. Figure 3 illustrates the ^{1}H NMR spectra of fractions obtained from a crude sample with an initial M_w of ~1600, ranging from the most volatile, essentially pure *b*-PIB to the nonvolatile, nearly pure *l*-PIB. The ^{1}H DOSY NMR spectrum of the fourth fraction in $CDCl_3$ (Figure 4) demonstrates that the carborate signals are not due to leftover impurity **1** but have the same diffusion coefficient as the polymer itself, $D = 3.8 \times 10^{-10}$ $m^2 \cdot s^{-1}$, a factor of 1.5 lower than that of the anion of **1** under the same conditions ($D = 5.6 \times 10^{-10}$ $m^2 \cdot s^{-1}$). With another sample of *l*-PIB, we found a factor of 1.9. The *l*-PIB fraction also shows ^{11}B NMR signals (Figure S3, Supporting Information) and there is no doubt that the carborate cage is attached covalently to the *l*-PIB chain. There is no indication of an analogous attachment to *b*-PIB.

Since quantitative separation is difficult, the fractions of *l*-PIB and *b*-PIB in crude polymer mixtures were determined by integration of ^{1}H NMR spectra. For run 2 in Table 1 and run 3 in Table 3, the crude samples were separated and properties of each fraction were studied by GPC with triple detection. The results are collected in Tables 1−4, which summarize the effects of reaction conditions on the results of the catalyzed polymerization of IB. Table 1 shows that the two initiators yield similar

Table 2. Effect of Concentration of 1 on Polymerization of IB[a]

run	concn of **1**, wt %	PIB, mg[b]	PIB composition[c]	M_w	MWD[d]
1	3	20	80% *l*-PIB	5900	2.2
	3	20	20% *b*-PIB	1000	1.4
2	10	60	90% *l*-PIB	32 000	2.7
	10	60	10% *b*-PIB	650	1.6
3	20	89	100% *l*-PIB	52 000	3.2

[a] DCE (0.5 mL), air (1 min of bubbling), 1 atm of IB, 24 h, 25 °C. [b] Total polymer yield. [c] Determined by ^{1}H NMR integration. [d] Molecular weight distribution.

Table 3. Effect of Solvent on Polymerization of IB[a]

run	solvent	PIB, mg[b]	PIB composition[c]	M_w	MWD[d]
1	DCE	60	90% *l*-PIB	32 000	2.7
	DCE	60	10% *b*-PIB	650	1.6
2	benzene	30	90% *l*-PIB	30 000	2.4
	benzene	30	10% *b*-PIB	2800	1.6
3	toluene	17	60% *l*-PIB	2000	1.9
	toluene	17	40% *b*-PIB	800	1.1
4	ether	8	10% *l*-PIB	3000	2.0
	ether	8	90% *b*-PIB	700	1.2

[a] Solvent (0.5 mL), **1** (50 mg), air 1 min bubbling, 1 atm of IB, 25 °C, 24 h. [b] Total polymer yield. [c] Determined by ^{1}H NMR integration. [d] Molecular weight distribution.

Table 4. Air-Initiated IB Polymerization in the Presence of Radical and Cation Traps[a]

run	solvent	additive, 50 mg	PIB, mg[b]	PIB	M_w	MWD[c]
1	DCE	C_{60}	320	*l*	7000	2.7
2	DCE	TEMPO	96	*l*	1700	1.3
3	benzene	LiO*t*Bu	6	*b*	580	1.2
4	benzene	methanol-d_4	35	*b*	520	1.3

[a] Solvent (0.5 mL), air 1 min bubbling, **1** (50 mg), 1 atm of IB, 25 °C, 24 h. [b] Total polymer yield. [c] Molecular weight distribution.

results. Table 2 demonstrates that at higher concentrations of **1** the polymerization activity, the portion of *l*-PIB in the polymer, and the molecular weight of *l*-PIB increase. Table 3 illustrates the effect of the solvent, which strongly influences the amount of polymer formed and can change its composition from almost exclusively linear to almost exclusively branched. Table 4 lists the effects of radical and cation trapping agents. Finally, Table 5 displays the effect of the content of sulfolane in **1** with air initiation. Sulfolane-free **1** has no catalytic action, and **1** that contains more than about 1 sulfolane molecule per Li^+ cation has very little activity. With air initiation in DCE, the maximum activity is found in the vicinity of a molar ratio sulfolane:$Li^+ \simeq$ (1−2):10 and the ratio 1.5:10 appears best. For the previously

Table 5. Influence of Sulfolane on Activity of 1[a]

run	mol of sulfolane/mol of Li^+	PIB, mg[b]	M_w	MWD[c]
1	0	0		
2	0.025	26	4000	1.8
3	0.05	48	26 000	2.7
4	0.1	60	32 000	2.7
5	0.15	51	29 000	2.8
6	0.3	48	26 000	2.7
7	1	27	8000	2.0
8	3	23	730	1.2

[a] Sulfolane was added to a solution of **1** (50 mg) in DCE (0.5 mL) immediately before the polymerization was started, air 1 min bubbling, 1 atm of IB, 25 °C, 24 h. [b] Total polymer yield. [c] Molecular weight distribution.

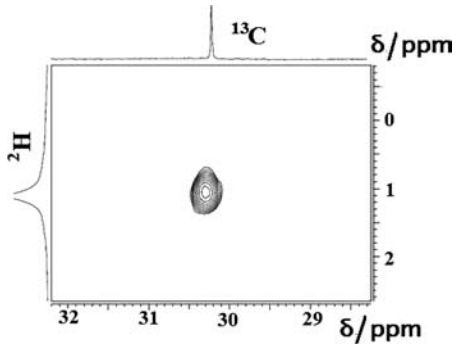

Figure 5. $^2H-^{13}C$ HetCorr NMR spectrum in $CHCl_3$ of *l*-PIB obtained from $CH_2{=}C(CD_3)_2$. Sample was similar to run 1 in Table 1.

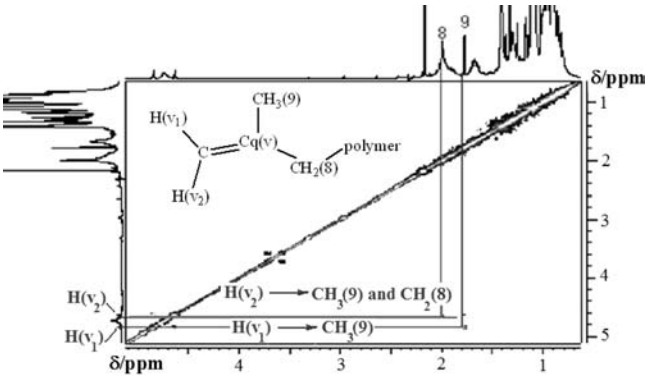

Figure 6. gCOSY ^1H NMR spectrum in $CDCl_3$ of *l*-PIB fraction from run 3 in Table 3.

reported[3] initiation with ATB in DCE, the results are similar and the best ratio was 1.7:10. In general, the optimal ratio is a function of solvent and, to some small degree, initiator, but it does not appear to depend on the nature of the monomer.[15]

Structure of *l*-PIB Backbone and Chain End. The unbranched $[\text{-}CH_2C(CH_3)_2\text{-}]_n$ backbone structure of the *l*-PIB produced is fairly obvious from its NMR spectra. We confirmed it by an additional experiment, in which $CH_2{=}C(CD_3)_2$ was polymerized under conditions similar to run 1 of Table 1. In the $^2H-^{13}C$ HetCorr NMR spectrum of the resulting *l*-PIB product, the deuterium signal was found only in the methyl region (Figure 5).

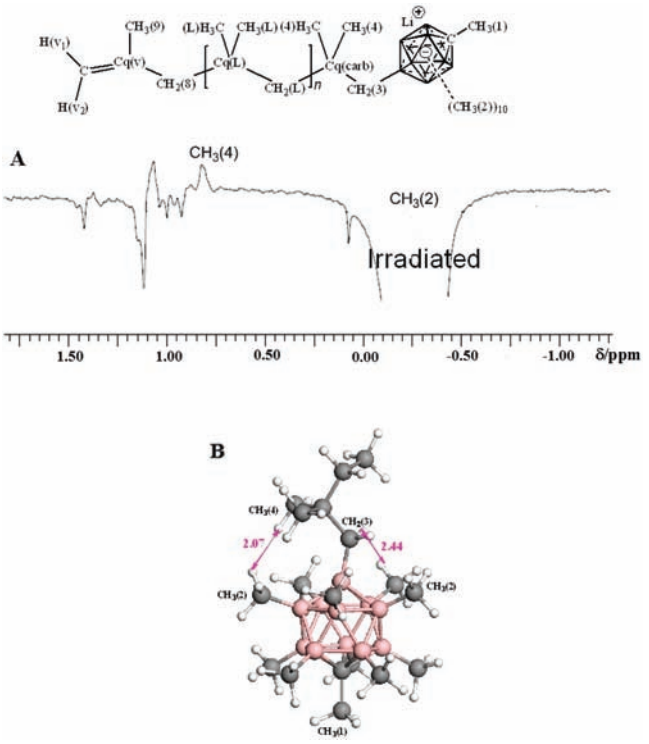

Figure 7. (A) Structure of *l*-PIB and NOE difference ^1H NMR in $CDCl_3$. (B) Distances between $CH_3(4)$ and $CH_3(2)$ and between $CH_2(3)$ and $CH_3(2)$.

In contrast, the nature of the chain ends remains to be determined. Since we had the ability to produce relatively low molecular weight samples, we were able to use several NMR methods to perform the determination. We found two distinct chain ends. One is the same isobutenyl that was found in *b*-PIB,[3] and the other is a carborate residue. The procedure is illustrated in Figures 4−8. In addition to the protons of the main chain, the DOSY spectrum in Figure 4 clearly shows the protons of the vinyl and carborate groups. The gradient COSY NMR spectrum (Figure 6) displays the interactions between vinyl protons v_1 and v_2 and protons of the methyl and methylene groups in the allylic positions of the isobutenyl residue.

The heteronuclear multiple bond correlation (HMBC) NMR spectrum (Figure S4 in Supporting Information) revealed the typical pattern of signals for the isobutenyl chain end and also helped to identify the signal of quaternary carbons in the linear part of the polymer chain. Both groups are marked in the spectrum and correspond well to data for the linear polymer produced by cationic polymerization and described previously in the literature.[16]

To examine the nature of the connection of the carborate anion to *l*-PIB, a NOE difference experiment was performed. The only signal that responded to the irradiation of all methyl groups of the carborate anion was that of the geminal methyls $CH_3(4)$, suggesting the structure shown in Figure 7. A molecular model, also displayed in Figure 7, demonstrates that the $CH_3(4)$ protons are closer to those of the carborate methyl groups than are the protons of the $CH_2(2)$ group directly attached to the B(12) vertex of the cage. We have no evidence for the choice of position 12 of the carborate cage for the attachment to the polymer chain,

dx.doi.org/10.1021/ja111659u | *J. Am. Chem. Soc.* 2011, 133, 7801–7809

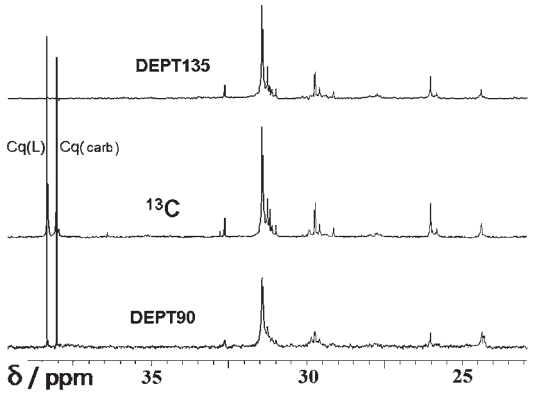

Figure 8. ^{13}C NMR spectrum and DEPT analysis in $CDCl_3$ of *l*-PIB from run 3 in Table 3.

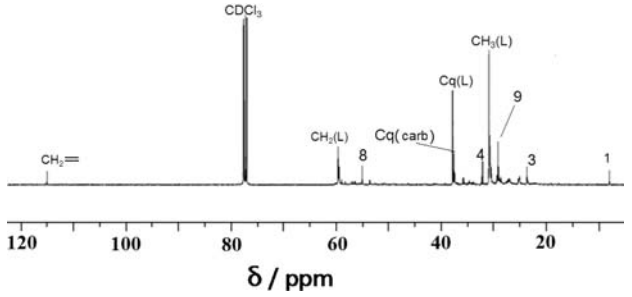

Figure 9. ^{13}C NMR spectrum of *l*-PIB in $CDCl_3$ with final assignments.

but it is likely that this generally most reactive position[17] is indeed the correct choice.

Figure 8 shows all quaternary carbons of the polymer that were revealed by comparison of the ^{13}C NMR spectra, where they are present, with DEPT 135 spectra, where they are absent. The results yield the assignments shown in Figure 8. The assignment for the main chain was confirmed by gradient HMBC NMR (Figure S4 in Supporting Information). One of the quaternary carbons of the backbone has a slightly but distinctly different chemical shift from the rest and has been tentatively assigned as the last quaternary carbon at the carborate chain end.

Gradient HSQC NMR with phase editing, which differentiates between methyl and methylene groups, was applied to confirm all the assignments. In particular, it firmed up assignments that were available only from ^1H NMR or only from ^{13}C NMR. Figure S5 (Supporting Information) shows the discrimination between methyl (red) and methylene (blue) groups.

Figure 9 summarizes the results obtained by all NMR methods and shows the final carbon atom assignments in the ^{13}C NMR of *l*-PIB with carborate chain end.

Triple Detection GPC. Two purified *l*-PIB samples, containing a carborate chain end according to NMR, were analyzed by triple-detection GPC. The triple-detection chromatogram of the *l*-PIB fraction isolated from run 2 in Table 1 is shown in Figure 10 (M_w = 6500). The measurement by RI detection and polystyrene standards yielded a relative value of 25 000 (the isolation and purification procedures may have contributed to the difference in molecular weights). This sample had rather narrow polydispersity (1.58), a relatively high M_z (9800), and relatively low intrinsic viscosity (0.14). The Mark−Houwink slope was 0.578. The second sample (run 3, Table 3) had a lower M_w (2500) but still

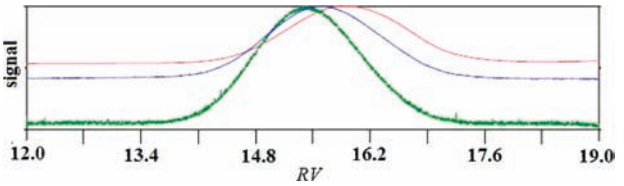

Figure 10. Triple-detection chromatogram of *l*-PIB with carborate chain end. Red, refractive index (RI) detector; green, light scattering (LS) detector; blue, intrinsic viscosity (IV) detector. *RV* is retention volume in milliliters.

has a relatively high M_z (4100) and relatively low intrinsic viscosity (0.09). Its Mark−Houwink slope was 0.522.

The fate of **1** in the IB polymerization process was examined by running the reaction in an NMR tube in DCE-d_2 under air initiation and taking ^{11}B NMR periodically. Decomposition became apparent after about 1 week when new NMR signals started to grow. After 2 weeks, the mixture was analyzed by MALDI-TOF with fullerene C_{60} as a matrix. By then, the initial light yellow color of the DCE solution had changed to dark brown. Negative ESI-MS showed a single major peak at m/z = 352, which fits structure **2** (n = 0) in Chart 1. We have no evidence that the long substituent is attached in position 12 as shown, and it was selected for the drawing merely because it usually is the most reactive. MALDI-TOF of the solution at the end of polymerization and after addition of C_{60}, known to be a radical trap[18−21] and a good matrix for MALDI-TOF,[22] indicated the formation of the same peak at m/z = 352, attributable to **2**, and its adduct with C_{60}, as well as several additional peaks. Their m/z ratios fit expectations for **3**, **4**, etc. These are analogues of **1** in which the methyl group in position 12 was replaced by short PIB chains of different lengths (Chart 1). At the end, no starting **1** was found by MALDI-TOF or by ESI-MS of the solution.

Initiation with $CB_{11}Me_{12}^{\bullet}$. The polymerization of IB in DCE in the presence of 10 wt % separately prepared pure $CB_{11}Me_{12}^{\bullet}$,[13] and in the absence of any other initiator or **1**, resulted in the formation of pure *l*-PIB and no *b*-PIB. ^1H NMR and DOSY demonstrated the presence of the usual carborate chain end.

When 10 wt % **1** was also present, the same experiment yielded only low-molecular weight *b*-PIB. When the CH_3 groups in positions 2−12 of the $CB_{11}Me_{12}^{\bullet}$ radical were replaced with CD_3, the experiment was repeated, and the oligomers were separated on Kugelrohr, deuterium was found by NMR in both the *b*-PIB and *l*-PIB products. In *b*-PIB, it appeared at 0.9 ppm and was assigned to a CD_3 chain end, and in *l*-PIB, it appeared in the carborate CD_3 region.

When *l*-PIB (M_w = ∼6000) with carborate at a chain end (run 1 in Table 2) and IB were exposed to the $CB_{11}Me_{12}^{\bullet}$ radical (15 wt %) and **1** (10 wt %) simultaneously, the reaction product was only *b*-PIB (M_w = ∼800). Figure 11 shows the ^1H NMR spectra of the *l*-PIB reactant and the *b*-PIB product. When commercial *l*-PIB (BASF 2300) carrying no carborate as a chain end was used in the same experiment, the degradation of *l*-PIB by the $CB_{11}Me_{12}^{\bullet}$/**1**/IB mixture was very much slower and the degree of branching in the product much lower. In another control experiment, a sample of the carborate-carrying *l*-PIB was exposed to the $CB_{11}Me_{12}^{\bullet}$ radical (15 wt %) alone, in the absence of **1** and IB. No changes in the *l*-PIB structure were detectable after 48 h.

Initiation with $CB_{11}Me_{11}$. When the borenium ylide $CB_{11}Me_{11}$ with a naked vertex 12 was prepared in situ at low temperature by reaction[14] of $CB_{11}Me_{12}^{\bullet}$ with t-Bu_6Si_2 and the crude

dx.doi.org/10.1021/ja111659u | J. Am. Chem. Soc. 2011, 133, 7801–7809

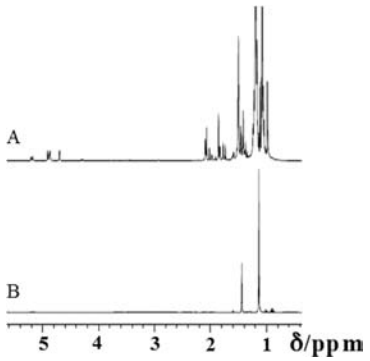

Figure 11. ^{1}H NMR spectra of *l*-PIB fraction from run 1 in Table 2 in $CDCl_3$, (B) before and (A) after reaction with $CB_{11}Me_{12}^{\bullet}$ and **1**.

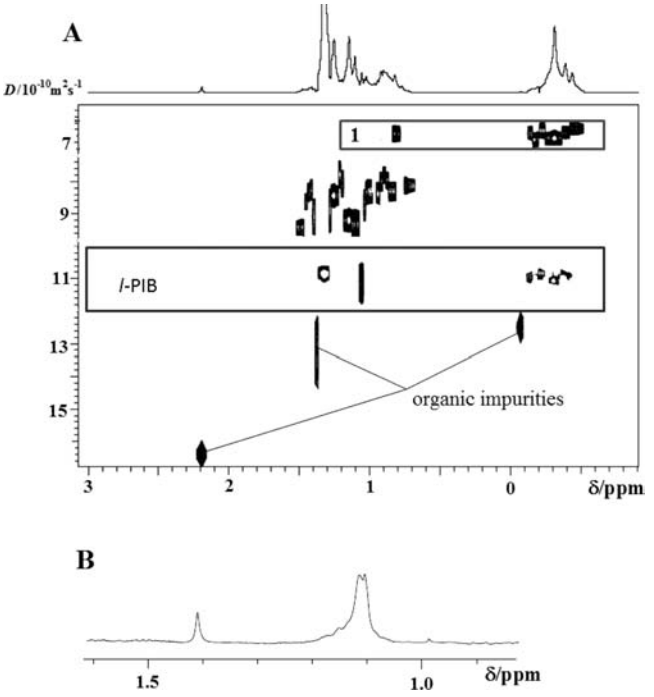

Figure 12. (A) ^{1}H DOSY NMR spectrum in liquid SO_2 of the reaction mixture from the polymerization of IB initiated with $CB_{11}Me_{11}$. (B) ^{1}H NMR spectrum of the isolated polymer.

reaction mixture was exposed to IB in hexane or liquid SO_2 at temperatures below −60 °C for 24 h, *l*-PIB was formed and ^{1}H DOSY NMR showed the presence of a carborate anion chain end (Figure 12).

DISCUSSION

With a nonoxidizing radical initiator such as ATB in a weakly ligating solvent and in the presence of a high concentration of **1** (∼10 wt %), IB undergoes a radical polymerization to a highly branched *b*-PIB polymer with a M_w in the thousands. The mechanism proposed for this process involves an acceleration of the propagation step relative to chain transfer by complexation of the IB monomer with Li^+.[3]

We now find that, with oxidizing radical initiators such as DTPB or air under otherwise identical conditions, a mixture of two distinct polymers is produced. One is the already-known[3] *b*-PIB, and the other is *l*-PIB with a M_w in the tens of thousands and with a carborate anion attached at the chain end. The amounts of linear and branched fraction formed vary from very low to very high depending on solvent, temperature, and the presence of additives (Tables 1−4). The polymerization activity grows with the concentration of **1** (Table 2) until the concentration approaches saturation (∼26% for DCE). A suitable working concentration is ∼10%, quite high for a catalyst. Since **1** is being incorporated into the polymer chain end, **1** is not only a catalyst but also a reagent.

There is no indication in the NMR spectra of the polymers that any chains containing both a *b*-PIB and an *l*-PIB part are formed. It thus appears that, unlike the nonoxidizing ATB, which initiates only a radical polymerization of IB to *b*-PIB, the oxidizing initiators examined presently apparently trigger a simultaneous radical polymerization of IB to *b*-PIB and its cationic polymerization to *l*-PIB. In the presence of radical traps only *l*-PIB is formed, whereas in the presence of cation traps only *b*-PIB is formed (Table 4).

The *b*-PIB product appears identical in all respects to the highly branched polymer produced previously with a nonoxidizing initiator.[3] The *l*-PIB product meets all standard expectations for a linear PIB, and one of its chain ends is the entirely unexceptional isobutenyl (Figure 7), the same as in the *b*-PIB product. The linear nature of this polymer follows from both NMR spectra and triple-detection GPC results. The retention times are nearly equal for all detectors, polydispersity is low, M_z is high, intrinsic viscosity is low, and the Mark−Houwink slope is characteristic of random coils and is very different from that typical of spherical molecules (cf. the slope of 0.1−0.2 for *b*-PIB).[3] The strictly linear dependence of log R_h on log M_w also fits expectations.

The only unusual aspect in which the *l*-PIB produced in our reaction differs from previously known *l*-PIB polymers is a chain end that carries a covalently attached carborate anion. The structure shown in Figure 7 was deduced from NMR data, which, however, do not discriminate among the possible points of attachment on the carborate cluster. The use of CD_3-labeled $CB_{11}Me_{12}^{\bullet}$ produced a sample with deuterium in the *b*-PIB and *l*-PIB fractions, in both cases in the chain end. In *b*-PIB it appeared as a terminal CD_3 group, and in *l*-PIB it appeared attached to the borons of the terminal carborate cage. All this is compatible with the structure shown in Figure 7 and suggests that at least some of the initiating Lewis acid was a carborate anion with a naked vertex, that is, the previously studied[14] strong Lewis acid, borenium ylide $CB_{11}Me_{11}$. The results of an experiment in which an authentic sample of $CB_{11}Me_{11}$ was shown to produce the same *l*-PIB product (Figure 12) and the MALDI-TOF results (Chart 1) are all compatible with this notion. We have drawn an attachment through the vertex 12, antipodal to the carbon, which is generally the most reactive, but we do not have definitive support for this choice.

How is the ylide generated, and how is the concurrent radical polymerization launched in the process? The reaction requires oxidizing conditions, and of all the constituents present, the carborate anion $CB_{11}Me_{12}^-$ is the most readily oxidizable species. Its redox potential is ∼1.15 V more positive than that of the ferrocene/ferricenium couple[23,24] and neither air nor DTBP is a strong enough oxidant to perform a stoichiometric oxidation (dibenzoyl peroxide is, and therefore it is not suitable as a radical initiator). However, it is easily imagined that even if the equilibrium is unfavorable, both air and DTBP are capable of oxidizing the anion to the radical

Scheme 1. Proposed Mechanism for Concurrent Formation of *b*-PIB and *l*-PIB

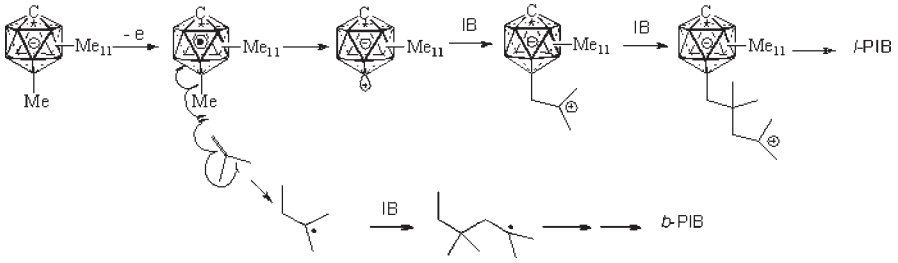

$CB_{11}Me_{12}^{\bullet}$ at a slow rate. If the radical were a source of the borenium ylide $CB_{11}Me_{11}$, it would be releasing it slowly and under conditions where it would not accumulate, since it would be rapidly consumed by the alkene present. Its low rate of release would then make it understandable that the M_w of the resulting *l*-PIB is so unusually high for the temperature used.

Results of experiments with the authentic radical $CB_{11}Me_{12}^{\bullet}$ established that it is indeed competent as a polymerization initiator for both cationic and radical processes. In the absence of **1**, the radical causes a conversion of IB to *l*-PIB, with the carborate attached to the chain end (Figure 12). No *b*-PIB was expected in the product, since without Li^+ catalysis, IB does not undergo radical polymerization, and none was observed. In the presence of **1**, the radical causes a conversion of IB to *b*-PIB, as anticipated, but the by now confidently expected concurrent formation of *l*-PIB was not observed. This puzzled us until we discovered that authentic *l*-PIB is not stable under the reaction conditions and is converted to *b*-PIB of much lower M_w. We shall return to this surprising observation below.

At this point, the only missing link is a facile conversion of the radical $CB_{11}Me_{12}^{\bullet}$ into the borenium ylide $CB_{11}Me_{11}$ in a fashion that is capable of simultaneously launching a radical polymerization chain. This requires the radical to act as a $CH_3^{\bullet}$ transfer agent. If $CH_3^{\bullet}$ were transferred from its position 12 (and possibly to some degree also others) to the terminal doubly-bonded carbon of IB, the products would be a *tert*-pentyl radical, $(C_2H_5)(CH_3)_2C^{\bullet}$, and borenium ylide, $CB_{11}Me_{11}$. As shown in Scheme 1, the former would then launch a radical polymerization chain and the latter, a cationic polymerization chain. The CD_3 labeling experiments supports this notion and we propose that this is just what happens.

There is precedent for $CB_{11}Me_{12}^{\bullet}$ acting as a $CH_3^{\bullet}$ transfer agent from position 12, in that it reacts with disilanes $R_3Si-SiR_3$ to yield the methylsilanes R_3SiCH_3.[14] The byproduct is $CB_{11}Me_{11}$ with a naked vertex in position 12, which is sufficiently stable in bulk for solid-state NMR characterization at low temperatures but decomposes upon warming.

The surprising conversion of *l*-PIB into *b*-PIB of lower M_w occurs very slowly even with commercial *l*-PIB that does not contain any carborate residues, but it is much faster with our *l*-PIB, which does. It requires the presence of **1**. A tentative mechanism for this degradation is proposed in Scheme 2. We suggest that the carborate anion at the chain end is first oxidized to a radical by electron transfer to $CB_{11}Me_{12}^{\bullet}$ and then fragments to produce, on the one hand, a $^{\bullet}CH_2-C(BMe_{11})^{\bullet}$ biradical whose electronic structure perhaps also contains ylide contributions of the type $^{+}CH_2-C(BMe)_{11}^{-}$, and on the other hand, a polymer chain-end radical that can unzip by repeated β-scission. The

Scheme 2. Proposed *l*-PIB Chain Degradation Mechanism in the Presence of $CCB_{11}Me_{12}$ Radical

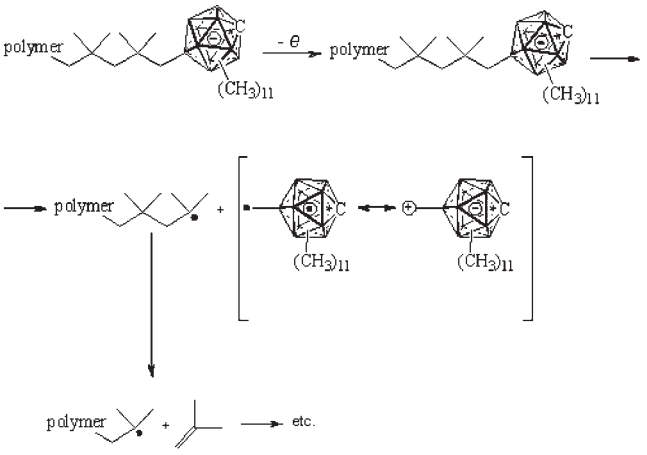

resulting IB joins the IB used as a reactant and polymerizes by the radical mechanism to yield *b*-PIB. In the absence of **1** and IB, no degradation of *l*-PIB was found, and this is compatible with Scheme 2. Even if IB is formed by the unzipping reaction, as demonstrated separately, in the presence of $CB_{11}Me_{12}^{\bullet}$ and absence of **1**, it can only polymerize back to *l*-PIB.

The hypothetical biradical $^{\bullet}CH_2-C(BMe)_{11}^{\bullet}$ can also be viewed as a deprotonated form of the *hypercloso*-carborane cation $MeC(BMe)_{11}^{+}$. We are presently trying to prepare these species electrochemically and characterize them computationally.[25]

The slow degradation of ordinary *l*-PIB, which contains no carborate chain ends, into low-M_w *b*-PIB by the simultaneous action of $CB_{11}Me_{12}^{\bullet}$ and **1** proceeds by an unknown mechanism and is currently under further investigation.

Although we believe that the present investigation has provided a solution to a puzzle, the concurrent radical and cationic polymerization of IB under the action of oxidizing initiators in the presence of **1**, it leaves several unanswered questions for future investigations. In addition to the just-discussed unknown mechanism of slow conversion of *l*-PIB to *b*-PIB that possibly involves previously unknown reactions and intermediates, it leaves open the exact nature of the species responsible for the catalytic properties of **1** in solvents of low polarity and the origin of the great sensitivity of these properties to the detailed composition of the solutions. A representative example of these uncertainties encountered in the present investigation is the absolute need for the presence of small but not excessive amounts of sulfolane in the reaction mixture (Table 5). It hints at a need to

dx.doi.org/10.1021/ja111659u | *J. Am. Chem. Soc.* 2011, 133, 7801–7809

loosen up otherwise tight aggregates in which the Li^+ cation is inaccessible and shows little if any activity.

SUMMARY

We have proposed a plausible mechanistic explanation for the puzzling observation that, in the presence of **1** in a solvent of low donicity, oxidizing radical initiators induce the concurrent polymerization of IB into *b*-PIB and *l*-PIB. Suitable additives can channel the reaction in one or the other direction. We found that the *l*-PIB formed carries a carborate anion at its chain end, and this makes it curiously susceptible to conversion to lower M_w *b*-PIB by combined action of IB, $CB_{11}Me_{12}^{\bullet}$, and **1**. We have proposed a tentative mechanism for initiating a linear chain unzipping process via a new type of biradical, $^{\bullet}CH_2-C(BMe)_{11}^{\bullet}$.

ASSOCIATED CONTENT

Supporting Information. List of abbreviations, five figures, and full ref 12. This material is available free of charge via the Internet at http://pubs.acs.org.

AUTHOR INFORMATION

Corresponding Author

michl@eefus.colorado.edu

Present Addresses

[‡]Department of Natural Sciences, School of Agricultural and Natural Sciences, University of Maryland Eastern Shore, Princess Anne, MD 21853.

ACKNOWLEDGMENT

We are grateful to the NSF (CHE-0715374) and the USARO (W911NF-08-1-0288 and W911NF-09-1-0124) for financial support, to Dr. Richard Shoemaker for assistance with NMR measurements and interpretations, to Ian M. Glassford for the preparation of samples of deuterated **1**, and to Jin Wen for computer modeling.

REFERENCES

(1) Vyakaranam, K.; Barbour, J. B.; Michl, J. *J. Am. Chem. Soc.* **2006**, *128*, 5610.
(2) Fendler, J. H. *Acc. Chem. Res.* **1976**, *9*, 153.
(3) Volkis, V.; Shoemaker, R.; Mei, H.; Michl, J. *J. Am. Chem. Soc.* **2009**, *131*, 3132.
(4) De, P.; Faust, R. In *Controlled and Living Polymerizations: From Mechanisms to Applications*; Müller, A. H. E., Matyjaszewski, K., Eds.; Wiley−VCH: Weinheim, Germany, 2009; p 57.
(5) Minsker, K. S.; Sangalov, Yu. A.; Zaikov, G. E. In *Physical Organic Chemistry: Theory and Practice*; D'Amore, A., Zaikov, G. E., Eds.; Nova Science: Hauppauge, NY, 2005; p 31.
(6) Nuyken, O.; Vierle, M. *Des. Monomers Polym.* **2005**, *8*, 91.
(7) Aoshima, S.; Kanaoka, S. *Chem. Rev.* **2009**, *109*, 5245.
(8) Mei, H.; Douvris, C.; Volkis, V.; Hanefeld, P.; Hildebrandt, N.; Michl, J. *Macromolecules* **2011**, *44*, 2558.
(9) Braunecker, W. A.; Akdag, A.; Boon, B. A.; Michl, J. *Macromolecules* **2011**, *44*, 1229.
(10) Janata, M.; Vlček, P.; Látalová, P.; Svitáková, R.; Kaleta, J.; Valášek, M.; Volkis, V.; Michl, J. *J. Polym. Sci. A, Polym. Chem.* **2011**, *49*, 2018.
(11) Franken, A.; King, B. T.; Rudolph, J.; Rao, P.; Noll, B. C.; Michl, J. *Collect. Czech. Chem. Commun.* **2001**, *66*, 1238.
(12) Frisch, M. J., et al. *Gaussian 09, Revision A.1*; Gaussian, Inc., Wallingford, CT, 2009.
(13) Clayton, J. R.; King, B. T.; Zharov, I.; Fete, M. G.; Volkis, V.; Douvris, C.; Valášek, M.; Michl, J. *Inorg. Synth.* **2010**, *35*, 56.
(14) Zharov, I.; Havlas, Z.; Orendt, A. M.; Barich, D. H.; Grant, D. M.; Fete, M. G.; Michl, J. *J. Am. Chem. Soc.* **2006**, *128*, 6089.
(15) Volkis, V.; Michl, J. Unpublished results.
(16) Tokles, M.; Keifer, P. A.; Rinaldi, P. L. *Macromolecules* **1996**, *28*, 3944.
(17) Körbe, S.; Schreiber, P. J.; Michl, J. *Chem. Rev.* **2006**, *106*, 5208.
(18) Bolton, J. R.; Wertz, J. E. *Electron Spin Resonance: Elementary Theory and Practical Applications*; Chapman and Hall: New York, 1986.
(19) Krusic, P. J.; Wasserman, E.; Keizer, P. N.; Morton, J. R.; Preston, K. F. *Science* **1991**, *254*, 1184.
(20) Tumanskii, B. L.; Kalina, O. G. *Radical Reactions of Fullerenes and Their Derivatives*; Kluwer Academic Publishers: Dordrecht, The Netherlands, 2001.
(21) Volkis, V; Tumanskii, B.; Eisen, M. S. *Organometallics* **2006**, *25*, 2722.
(22) Bonoldi, L.; Abis, L.; Fiocca, L.; Fusco, R.; Longo, L.; Simone, F.; Srea, S. *J. Mol. Catal. A: Chem.* **2004**, *219*, 47.
(23) King, B. T.; Körbe, S.; Schreiber, P. J.; Clayton, J.; Němcová, A.; Havlas, Z.; Vyakaranam, K.; Fete, M. G.; Zharov, I.; Ceremuga, J.; Michl, J. *J. Am. Chem. Soc.* **2007**, *129*, 12960.
(24) King, B. T.; Janoušek, Z.; Grüner, B.; Trammel, M.; Noll, B. C.; Michl, J. *J. Am. Chem. Soc.* **1996**, *118*, 3313.
(25) Wahab, A.; Ludvík, J.; Buchanan, E.; Michl, J. Unpublished results.